CHEMISTRY
A EUROPEAN JOURNAL

DOI: 10.1002/chem.200901883

Quinobis(imidazolylidene): Synthesis and Study of an Electron-Configurable Bis(N-Heterocyclic Carbene) and Its Bimetallic Complexes

Andrew G. Tennyson, Robert J. Ono, Todd W. Hudnall, Dimitri M. Khramov, Joyce A. V. Er, Justin W. Kamplain, Vincent M. Lynch, Jonathan L. Sessler,* and Christopher W. Bielawski*[a]

Abstract: Reaction of bromanil with *N*,*N*′-dimesitylformamidine followed by deprotonation with $NaN(SiMe_3)_2$ afforded 1,1′,3,3′-tetramesitylquinobis(imidazolylidene) (**1**), a bis(N-heterocyclic carbene) (NHC) with two NHC moieties connected by a redox active *p*-quinone residue, in 72% yield of isolated compound. Bimetallic complexes of **1** were prepared by coupling to FcN_3 (**2**) or FcNCS (**3**; Fc = ferrocenyl) or coordination to [M(cod)Cl] (**4a** or **4b**, where M = Rh or Ir, respectively; cod = 1,5-cyclooctadiene). Treatment of **4a** and **4b** with excess CO(g) afforded the corresponding $[M(CO)_2Cl]$ complexes **5a** and **5b**, respectively. Analysis of **2**–**5** by NMR spectroscopy and X-ray diffraction indicated that the electron-deficient quinone did not significantly affect the inherent spectral properties or coordination chemistry of the flanking imidazolylidene units, as compared to analogous NHCs. Infrared spectroscopy and cyclic voltammetry revealed that decreasing the electron density at ML_n afforded an increase in the stretching energy and a decrease in the reduction potential of the quinone, indicative of metal–quinone electronic interaction. Differential pulse voltammetry and chronoamperometry of the metal-centered oxidations in **2**–**4** revealed two single, one-electron peaks. Thus, the metal atoms bound to **1** are oxidized at indistinguishable potentials and do not appear electronically coupled. However, the metal–quinone interaction was used to increase the electron density at coordinated metal atoms. Infrared spectroelectrochemistry revealed that the average ν_{CO} values for **5a** and **5b** decreased by 14 and 15 cm^{-1}, respectively, upon reduction of the quinone embedded within **1**. These shifts correspond to 10 and 12 cm^{-1} decreases in the Tolman electronic parameter of this ditopic ligand.

Keywords: bimetallic complexes · carbene ligands · electrochemistry · ligand design · quinones

Introduction

From enantioselective synthesis[1] to the production of dihydrogen,[2] bimetallic catalysts have been employed in a variety of applications. Organometallic systems bearing N-heterocyclic carbene (NHC) ligands are useful catalysts for functional-group transformations and polymerization reactions,[3–13] and complexes featuring multitopic NHCs have recently emerged[14] as promising candidates for asymmetric and tandem catalysis,[15–17] as well as other applications.[18,19] Variants featuring two NHC moieties linked by a π-conjugated system, such as benzobis(imidazolylidene) (**BBI**),[20,21] triazolyldiylidene (**A**),[22] bitriazolylidene (**B**),[23] pyridylbis(imidazolylidene) (**C**),[24–26] and pyridazinylbis(imidazolylidene) (**D**)[27,28] have found numerous uses as ditopic ligands (Scheme 1). For example, **BBI**s have yielded phosphorescent complexes,[29] polymeric catalysts,[30] emissive and conducting polymers,[21,31–33] and self-assembled materials.[34,35] The π-systems linking the NHC units in **BBI** and **A**–**D** enable metal–metal interactions that can potentially modify the existing characteristics of the individual metal atoms (e.g., catalytic activity or phosphorescence) or create materials that exhibit new physical properties or functions altogether.

In nature, the reactivity of a bimetallic active site is often controlled through alteration of the stereoelectronic environment, such as ligand rearrangement or protonation/deprotonation.[36–40] A synthetic bimetallic complex lacks the secondary coordination sphere that enzymes employ to encapsulate and stabilize metal–ligand geometries, and there-

[a] Dr. A. G. Tennyson, R. J. Ono, Dr. T. W. Hudnall, Dr. D. M. Khramov, J. A. V. Er, Dr. J. W. Kamplain, Dr. V. M. Lynch, Prof. J. L. Sessler, Prof. C. W. Bielawski
Department of Chemistry & Biochemistry
The University of Texas at Austin
Austin, TX 78712 (USA)
E-mail: sessler@cm.utexas.edu
bielawski@cm.utexas.edu

Supporting information for this article is available on the WWW under http://dx.doi.org/10.1002/chem.200901883.

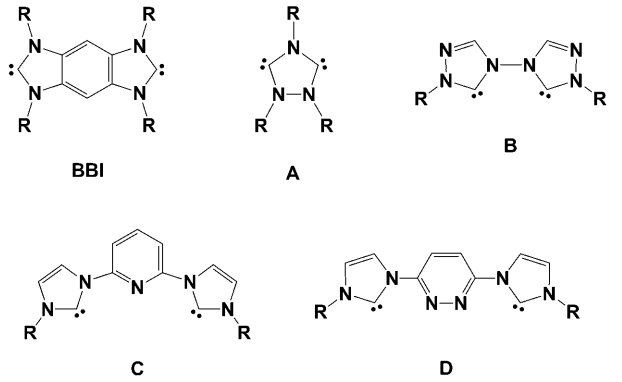

Scheme 1. Ditopic NHCs with π-conjugated linkers. For **BBI**, R = bulky alkyl or aryl.

fore analogous tuning in small molecules is difficult to achieve, particularly in a reversible manner. Electron-configurable ligands (i.e., those that undergo a reversible redox change to alter their electron-donating/withdrawing character) are attractive alternatives, given that electrochemical reversibility can be easily evaluated by cyclic voltammetry (CV).[41] Furthermore, many chemical redox agents with a wide range of potentials are known and often commercially available.[42] Complexes featuring electron-configurable ligands have yielded invaluable contributions to fields that range from fundamental studies of metal–ligand electronic interactions to practical redox-switchable catalysis.[43–49] Bimetallic variants comprising redox-active ditopic linkers have also been reported (Scheme 2),[50–55] such as tetrathiafulvene (**E**), *p*-quinonediphosphine (**F**), and quinodiimine (**G**). However, many of these scaffolds are highly specialized and difficult to modify; thus incorporating electron donating/withdrawing or solubilizing substituents into these systems can be synthetically challenging.

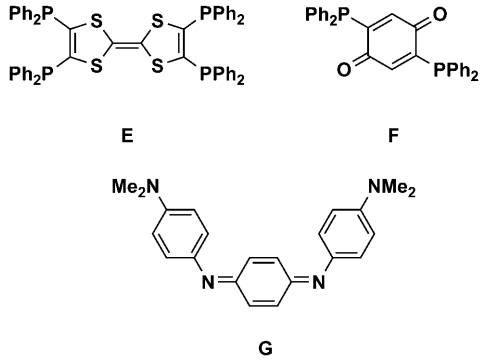

Scheme 2. Examples of redox-active ditopic ligands.

Unlike the aforementioned redox active ditopic ligands, **BBI**s and other ditopic NHCs can be synthesized and readily modified to exhibit a range of solubilities and stereoelectronic properties.[56] Inspired by these advantages, we previously showed that redox active groups can be built into NHCs, whereby redox changes thereof can be used to tune the electronic properties of coordinated metal atoms.[57,58] Initial efforts focused on the monotopic **NqMes** (Scheme 3), a napthoquinone-annulated 1,3-dimesitylimidazolylidene, which enabled fundamental studies of metal–NHC interactions[58–60] and new redox-switchable catalysts.[61] Because the **BBI** scaffold has been successfully employed in a range of applications,[21,29,31–33,35] we envisioned that a variant incorporating an electroactive group could potentially enable redox-switchable control over the intrinsic properties of these materials. We reasoned that a ditopic analogue of **NqMes** could be obtained by replacing the benzo linker in **BBI** with a *p*-quinone moiety by similar synthetic methods, thus affording an electron-configurable bis-NHC that combines the electronic tunability of **NqMes** with the structural versatility of the **BBI** scaffold.

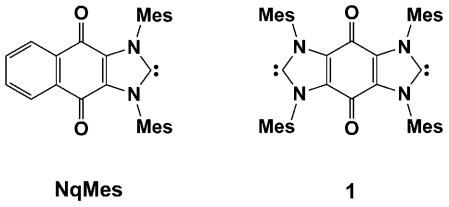

Scheme 3. Structures of electron-configurable NHCs.

Herein we report the synthesis of 1,1′,3,3′-tetramesitylquinobis(imidazolylidene) (**1**, Scheme 3) and investigations into the structural and electronic properties of bimetallic complexes thereof. We employed NHC coupling chemistry[62,63] to affix ferrocene (Fc) groups,[64] given that Fc displays well-defined electrochemical behavior. Additionally, we synthesized coordination complexes of **1** featuring [M(cod)Cl] and [M(CO)$_2$Cl] (M = Rh or Ir, cod = 1,5-cyclooctadiene) units. To explore how metal coordination affects quinobis(imidazolylidene) (QBI) electron density, the quinone stretching energies and reduction potentials in these complexes were analyzed by IR spectroscopy and electrochemistry. Similarly, metal oxidation potentials and carbonyl stretching frequencies were measured to ascertain the electron-donating ability of **1** to coordinated ML$_n$ units. Subsequent spectroelectrochemical IR analyses of quinone/carbonyl stretching energies upon metal oxidation and ligand reduction, respectively, provided insight into the electronic interactions[65] between the quinone in **1** and coordinated metal atoms. We found that **1** exhibits the coordination chemistry of a **BBI**, but increases electron density at bound ML$_n$ units upon reduction of the quinone moiety.

Results and Discussion

Condensation of bromoanil with four equivalents of *N*,*N*′-dimesitylformamidine in CH_3CN afforded bis-azolium [**1**H$_2$]

$[Br]_2$ in excellent yield (91%, Scheme 4). While other bases could be used to trap the HBr generated by this double-Michael addition, the best yields were obtained by using an excess of formamidine as the sacrificial base.[66,67] Although $[\mathbf{1}H_2][Br]_2$ served as the synthetic precursor for **1**, poor solubility even in polar organic solvents, such as CH_3CN or DMSO, precluded detailed electrochemical analyses (vide infra). To enhance organic solubility of the bis-azolium, anion exchange[68] was effected by treating $[\mathbf{1}H_2][Br]_2$ with MeOTf (OTf = CF_3SO_3), affording $[\mathbf{1}H_2][OTf]_2$ (eliminating volatile CH_3Br) in high yield (94%). The ^{13}C NMR signals for the quinone carbon atoms and those in the 2,2′-positions in $[\mathbf{1}H_2][Br]_2$ ($\delta = 163.7$ and 141.2 ppm, respectively) and $[\mathbf{1}H_2][OTf]_2$ ($\delta = 164.9$ and 143.7 ppm, respectively; Table 1) agreed with those of napthoquinone-annulated imidazolium chloride [**NqMes**H][Cl] ($\delta = 173.4$ and 141.8 ppm, respectively).[58] Structural assignment of $[\mathbf{1}H_2][OTf]_2$ was confirmed by X-ray diffraction (see Figure S1 in the Supporting Information). This complex has an N1-C2-N2 angle of 110.2(3)° (Table 1),[69] which compares well to that of [**NqMes**H][Cl] (108.07(14)°)[58] and analogous values observed in other benzimidazolium-derived compounds (110.1–111.7°).[20,70–76]

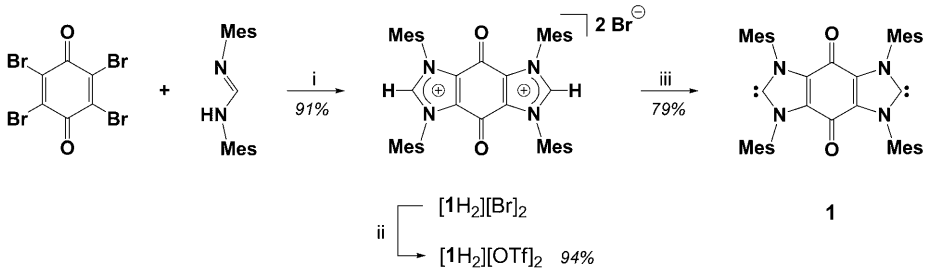

Scheme 4. Synthesis of **1**. i) 4 equiv *N,N′*-dimesitylformamidine, CH_3CN, 110°C, 24 h. ii) Excess MeOTf, CH_2Cl_2, RT, 2 h. iii) 2 equiv $NaN(SiMe_3)_2$, THF, RT, 30 min.

Table 1. Selected spectroscopic and structural data.

	$\delta(C^{2,2'})$ [ppm]	$\delta(C^{4,4'})$ [ppm]	ν_{CO} [cm^{-1}][d]	N-C-N [°][e]
$[\mathbf{1}H_2][OTf]_2$[a]	143.7	164.9	1710	110.2(3)
1[b]	232.6	168.0	1676	102.3(3)
2[c]	150.5	164.9	1662	105.7(5)
3[c]	141.2	171.1	1692	108.0(4)
4a[c]	201.0	164.5	1680	104.11(16)
4b[c]	195.3	164.9	1678	104.14(17)
5a[c]	193.0	164.1	1688	–[f]
5b[c]	188.7	164.1	1686	–[f]

[a] ^{13}C NMR measurements performed in CD_3CN. [b] ^{13}C NMR measurements performed in [D_8]THF. [c] ^{13}C NMR measurements performed in $CDCl_3$. [d] Quinone stretching energies ν_{CO} measured in KBr matrices. [e] This metric parameter is sensitive to the electronic environment at the QBI 2,2′-positions. [f] Not determined.

Deprotonation of $[\mathbf{1}H_2][Br]_2$ with $NaN(SiMe_3)_2$ afforded quinobis(imidazolylidene) **1** in good yield (79%). Compound **1** was also prepared from $[\mathbf{1}H_2][OTf]_2$ in comparable yields. The diagnostic ^{13}C signal for the 2,2′-positions in **1** was significantly downfield ($\delta = 232.6$ ppm, [D_8]THF, Table 1), but in accord with those of other NHCs ($\delta =$ 205.9–244.5 ppm)[20,70,76–79] and similar to that of **NqMes** ($\delta =$ 231.7 ppm, C_6D_6).[58] The structure of **1** was confirmed by X-ray analysis (Figure 1). The N-C-N angle observed in **1** (102.3(3)°, Table 1) was nearly identical to that of **NqMes** (102.1(6)°) and slightly more acute than those of known **BBI**s (R = Ad or *t*Bu, 104.4–104.8°).[20] Presumably, the acute N-C-N angle observed in **1** reflects the smaller steric bulk of mesityl versus tertiary alkyl groups.[80] Given the similar N-C-N angles in **1** and 1,3-dimesitylimidazolylidene (**IMes**) of 102.3(3) and 101.4(3)°, respectively,[81] the QBI could be viewed as two **IMes** fragments annulated by *p*-quinone.

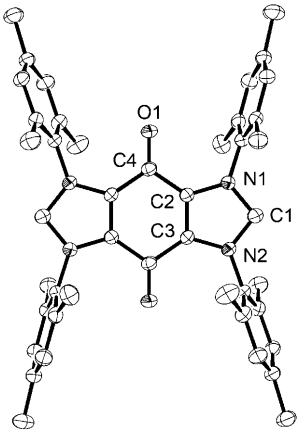

Figure 1. ORTEP showing 50% probability thermal ellipsoids and selected atom labels for **1**. Hydrogen atoms and solvent molecules have been omitted for clarity. Selected bond lengths [Å] and angles [°]: N1–C1, 1.375(4), N2–C1, 1.378(4), N2–C3, 1.386(4), O1–C4, 1.218(4), C2–C3, 1.367(4), C2–C4, 1.476(4); N1-C1-N2, 102.3(3).

To explore the coordination chemistry and electronic properties of **1**, we envisioned using electrochemical techniques to probe the metal-to-ligand and ligand-to-metal electronic interactions. Thus, we sought to affix redox active ML_n units to the redox active QBI by capitalizing on the reactivity of NHCs toward electrophiles.[62,63] Given that ferrocene (FcH) can be functionalized[64] with NHC-reactive moieties and exhibits well-defined electrochemical behavior, we pursued derivatives bearing groups that would facilitate coupling to **1**. Previously, we attached Fc-based electrochemical handles to **BBI** (R = *tert*-amyl) by using NHC–azide[82] and NHC–isothiocyanate[62] coupling chemistry to afford adducts **II** and **III**, respectively (Scheme 5).[83] Electrochemical anal-

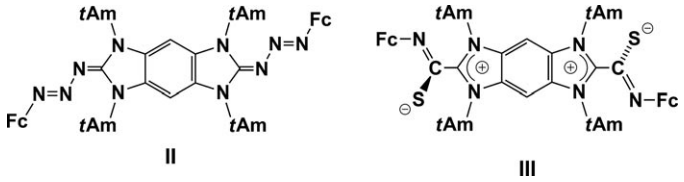

Scheme 5. Previously reported **BBI** adducts of FcN_3 (**II**) and FcNCS (**III**).

ysis of **II** revealed electronic coupling between the two metal centers, whereby oxidation of one ferrocene unit shifted that of the other to a higher potential ($\Delta E_{1/2} = 0.14$ V). Conversely, **III** only displayed one redox couple, indicating that the iron centers are oxidized at indistinguishable[84] potentials and do not interact. The lack of electronic coupling between metal atoms in **III** was attributed to the NCS linkage being orthogonal to the **BBI**, thus interrupting conjugation.

To prepare QBI-supported analogues of **II** and **III** and enable similar electrochemical investigations, we combined **1** with 2 equiv of FcN_3 or FcNCS to obtain the desired adducts $[(FcN_3)_2(\mathbf{1})]$ (**2**) or $[(FcNCS)_2(\mathbf{1})]$ (**3**) in modest yields (54 and 51%, respectively, Scheme 6). Consistent with the loss of carbenoid character, the ^{13}C NMR signal for the 2,2′-positions of these compounds had shifted significantly from $\delta = 232.6$ ppm in **1** ([D$_8$]THF) to 150.5 and 141.8 ppm in **2** and **3** ($CDCl_3$), respectively (Table 1). Structural confirmation of **2** and **3** was achieved by crystallographic analysis (see Figures 2 and 3, respectively).

To investigate how **1** interacts with FcN_3 and FcNCS relative to a **BBI**, we compared the metric parameters of **2** and **3** to **BBI**-supported analogues **II** and **III**. The N-C-N angles in **2** and **3** were found to be 105.7(5) and 108.0(4)° (Figure 2

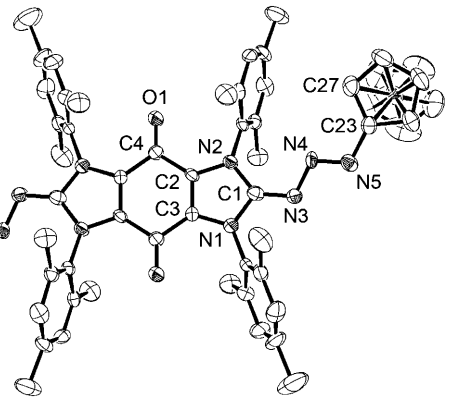

Figure 2. ORTEP showing 50% probability thermal ellipsoids and selected atom labels for **2**. Hydrogen atoms and solvent molecules have been omitted for clarity. Selected bond lengths [Å] and angles [°]: N1−C1 1.381(7), N2−C1 1.392(7), N3−C1 1.316(7); N1-C1-N2 105.7(5), N3-N4-N5 110.5(5), N2-C1-N3-N4 17.3(9), N4-N5-C23-C27 165.4(8).

and Figure 3, as well as Table 1), slightly more acute than those found in **II** and **III**, reflecting the different N-C-N geometries induced by aryl versus bulky *N*-alkyl substituents. Because the N-C-N bond angle in **3** is greater than that in **2** and comparable to that of $[\mathbf{1}H_2][OTf]_2$, we conclude that the QBI core in **3** bears significant positive charge and thus has zwitterionic character, consistent with **III**.[83] Whereas the triazene linkers in **2** are nearly coplanar with the QBI core (N2-C1-N3-N4 17.3(9)°), the isothiocyanate groups in **3** are nearly perpendicular (N1-C1-C5-S1 88.7(6)°), that is, geometries similar to those observed in **II** and **III** (31.3(6) and 92.6(5)°, respectively).[83] Presumably, the triazene units are more coplanar with the QBI in **2** than the **BBI** in **II** due to diminished steric crowding of the *N*-mesityl substituents. Furthermore, the internal angles for triazene and isothiocyanate linkages in **2** and **3** (110.5(5) and 136.5(4)°, respectively) are nearly identical to those observed in **II** and **III** (110.3(3) and 135.3(3)°, respectively). Because **1** forms adducts with FcN_3 and FcNCS that are comparable to their **BBI**-supported analogues, we conclude that the reactivity of the imidazolylidene moieties in **1** is preserved despite their being linked by a redox-active quinone moiety.

After verifying that **1** engaged in NHC–electrophile coupling chemistry, we sought to explore the coordination chemistry of this bis-NHC by affixing [M(cod)Cl] units (M = Rh or Ir) to **1**, chosen for their well-studied spectroscopic and structural properties in other

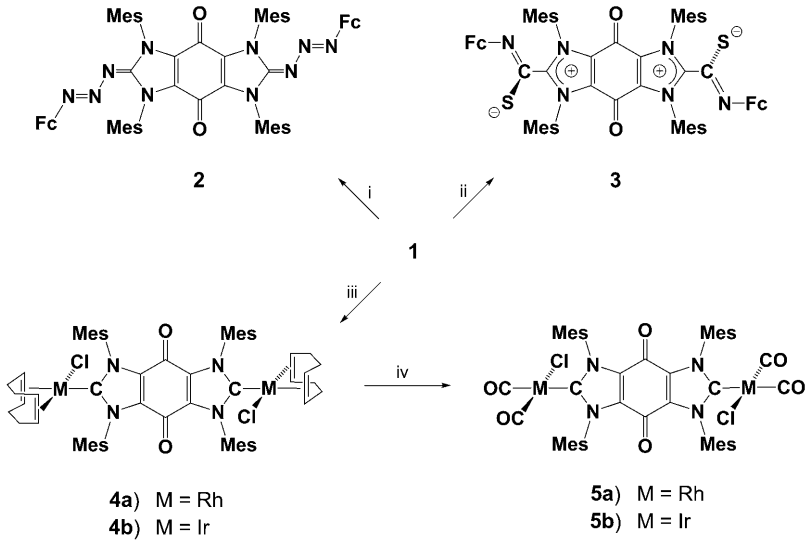

Scheme 6. Syntheses of complexes **2**–**5**. i) 2 equiv FcN_3, THF, 16 h, 54% yield. ii) 2 equiv FcNCS, toluene, 16 h, 51% yield. iii) 1 equiv $[M(cod)Cl]_2$, THF, 16 h (M = Rh or Ir for **4a** and **4b** in 69 and 64% yield, respectively). iv) 1 atm CO(g), CH_2Cl_2, 30 min, 91 and 93% yield for **5a** and **5b**, respectively.

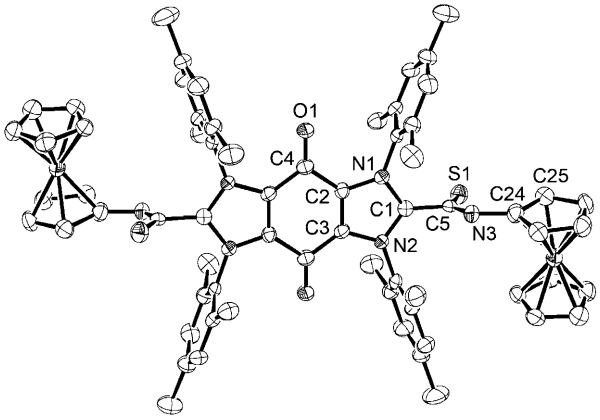

Figure 3. ORTEP showing 50% probability thermal ellipsoids and selected atom labels for **3**. Hydrogen atoms and solvent molecules have been omitted for clarity. Selected bond lengths [Å] and angles [°]: N1−C1 1.360(7), N2−C1 1.351(6), S1−C5 1.706(6), C1−C5 1.486(7); N1-C1-N2 108.0(4), S1-C5-N3 136.5(4), N1-C1-C5-S1 88.7(6), C25-C24-N3-C5 16.5(10).

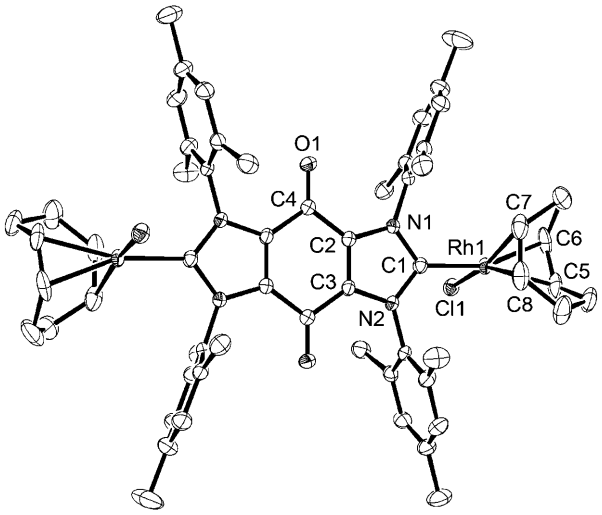

Figure 4. ORTEP showing 50% probability thermal ellipsoids and selected atom labels for **4a**. Hydrogen atoms and solvent molecules have been omitted for clarity. Selected bond lengths [Å] and angles [°]: N1−C1 1.376(3), N2−C1 1.376(3), C1−Rh1 2.033(2), Rh1−C5 2.224(2), Rh1−C6 2.198(2), Rh1−C7 2.127(2), Rh1−C8 2.103(2); N1-C1-N2 104.11(16), N1-C1-Rh1-Cl1 101.88(17). The cod bite angle is 86.5°.

NHC-supported complexes.[85–89] Furthermore, [M(cod)Cl] units are easily converted to $[M(CO)_2Cl]$, enabling investigation of the electron density at the metal center by IR spectroscopic analysis of the CO stretching frequencies.[85,86] Reaction of **1** with $[M(cod)Cl]_2$ in THF afforded bimetallic complexes $[\{M(cod)Cl\}_2(\mathbf{1})]$ (**4a**, M = Rh; **4b**, M = Ir) in good yields (69 and 64% yield, respectively; Scheme 6). The ^{13}C NMR signal for the 2,2′-positions in **4a** found at $\delta =$ 201.0 ppm ($J_{RhC} = 53.1$ Hz in $CDCl_3$, Table 1) was upfield relative to **1** ($\delta = 232.6$ ppm in $[D_8]$THF), but consistent with those of other [Rh(cod)Cl] complexes supported by NHCs, including **NqMes** ($\delta = 180.6$–225.8 ppm; $J_{RhC} = 41$–76 Hz).[57–59,70,85,90–94] Similarly, the ^{13}C signal for the 2,2′-positions in **4b** ($\delta = 195.3$ ppm; $CDCl_3$) was in good agreement with those reported for other NHC-supported [Ir(cod)Cl] complexes ($\delta = 179.6$–208.2 ppm).[22,70,87,93,94]

Crystals of **4a** suitable for X-ray diffraction enabled structural confirmation (Figure 4). A structure of the Ir congener suitable for publication could not be obtained due to twinning. The Rh1−C1 distance of 2.033(2) Å in **4a** is within the range of rhodium–NHC bond lengths observed in analogous **BBI** complexes (2.003–2.073 Å)[20] and monometallic NHC-supported variants (2.00–2.09 Å).[22,57,59,90,92,94–96] In addition, the average *cis* and *trans* rhodium–olefin distances in **4a** (2.115 and 2.211 Å, respectively) are comparable to those observed in the **BBI**-based variants (2.128–2.190 and 2.110–2.207 Å for *cis* and *trans* positions, respectively) and consistent with the Rh–cod bond lengths in monometallic NHC-supported analogues (2.09–2.23 Å).[22,57,59,90,92,94–96] Furthermore, the bite angle of the cod ligand in **4a** (86.5°) is within the range of values for NHC-supported [Rh(cod)Cl] complexes (85–89°).

Independently treating **4a** and **4b** with excess CO(g) afforded $[\{Rh(CO)_2Cl\}_2(\mathbf{1})]$ (**5a**) and $[\{Ir(CO)_2Cl\}_2(\mathbf{1})]$ (**5b**), respectively, in near-quantitative yields (Scheme 6). The ^{13}C NMR signals for the 2,2′-positions changed from $\delta =$ 201.0 and 195.3 ppm (in $CDCl_3$) in **4a** and **4b** to $\delta = 193.0$ and 188.7 ppm ($CDCl_3$) in **5a** and **5b** (Table 1), respectively, upfield shifts consistent with those of analogous **NqMes**-supported complexes.[58] Although single crystals of **5a** were obtained (Figure 5), diffraction-quality crystals of **5b** remained elusive. The Rh1−C1 distance in **5a** (2.067(4) Å) is within the range of values reported for other NHC-supported $[Rh(CO)_2Cl]$ complexes (2.06–2.09 Å).[95,96] Furthermore, the rhodium–carbonyl and C−O bond lengths measured *cis* (1.787(7) and 1.065(9) Å, respectively) and *trans* (1.890(5) and 1.113(8) Å, respectively) to the NHCs in **5a** compare

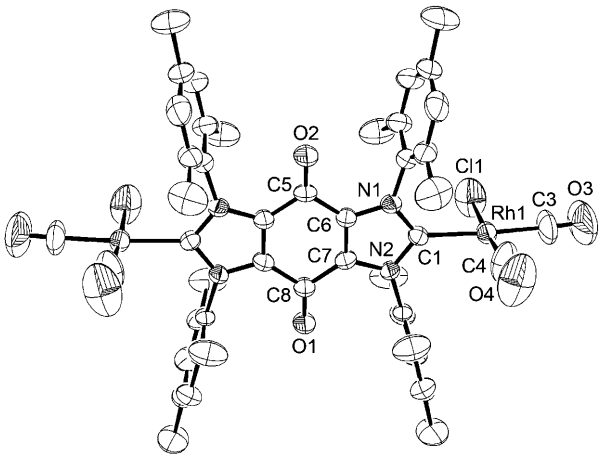

Figure 5. ORTEP showing 50% probability thermal ellipsoids and selected atom labels for **5a**. Hydrogen atoms and solvent molecules have been omitted for clarity. Selected bond lengths [Å] and angles [°]: N1−C1 1.354(11), N2−C1 1.372(11), O3−C3 1.115(9), O4−C4 1.067(10), C1−Rh1 2.063(5), Rh1−C3 1.889(6), Rh1−C4 1.776(8); N1-C1-N2 104.14(17), N1-C1-Rh1-Cl1 92.5(6).

well to the range of Rh–CO (1.84–1.88 Å and 1.90–1.91 Å for the *cis* and *trans* positions, respectively) and C–O (1.065(9) and 1.113(8) Å, respectively) distances observed in similar complexes supported by NHCs.[95,96] Given that the structural features of [Rh(cod)Cl] or [Rh(CO)$_2$Cl] fragments coordinated to **1** agree well with those bound by other NHCs, we conclude that the Rh–NHC interactions are comparable. Collectively, the spectral and structural similarities between **4** and **5** as well as other NHC-supported [M(cod)Cl] and [M(CO)$_2$Cl] complexes indicate that the quinone linker does not perturb the fundamental coordination chemistry of the two imidazolylidene units.

After studying the structural and spectroscopic features of the ML$_n$ units bound to **1**, we sought to measure the electron density within the QBI scaffold via IR spectroscopic analysis of the quinone carbonyl functional groups. As the system becomes more electron deficient, the ν_{CO} (quinone) value should increase (e.g., cyanil > chloranil > *p*-quinone > duroquinone).[97–99] Of all the compounds investigated, [**1**H$_2$]-[Br]$_2$ and [**1**H$_2$][OTf]$_2$ displayed the highest values for ν_{CO} in KBr at 1708 and 1710 cm^{-1} (Table 1), respectively, consistent with these molecules being the most electron deficient due to their dicationic nature. Deprotonation to form **1** resulted in a substantial shift in ν_{CO} to lower energy (1676 cm^{-1} in KBr), reflecting the greater electron density within the neutral bis-carbene, and it agrees well with the value observed in **NqMes** (1671 cm^{-1} in KBr).[58] Whereas the solid-state quinone stretching frequency for triazene **2** (1662 cm^{-1}) was slightly lower in energy than that of **1**, the ν_{CO} value for isothiocyanate adduct **3** (1692 cm^{-1}) was significantly higher, that is, FcN$_3$ donates electron density to **1**, and FcNCS is effectively electron-withdrawing. Consistent with its proposed zwitterionic formulation, the ν_{CO} (quinone) for **3** is closest in energy to that observed for [**1**H$_2$][OTf]$_2$.

Although adducts **2** and **3** exhibit significant disparity in quinone stretching energies, bimetallic complexes **4** and **5**, featuring metal atoms bound directly to the NHC moieties, display a narrower range of ν_{CO} (quinone) values (1678–1688 cm^{-1}; see Table 1). For **4a** and **5a**, the ν_{CO} (quinone) values of 1680 and 1688 cm^{-1} in KBr, respectively, reflect the weaker electron-withdrawing character of [Rh(cod)Cl] compared to [Rh(CO)$_2$Cl] and are in good agreement with the values observed for the **NqMes**-supported analogues (1670 and 1680 cm^{-1} in KBr, respectively).[58] Interestingly, the ν_{CO} (quinone) for congeners **4b** and **5b** occurred at slightly lower energies in the solid-state (1678 and 1686 cm^{-1}, respectively), consistent with the better π-backbonding ability of Ir relative to Rh (a consequence of the slightly lower electronegativity and larger ionic radius of the former).[100] Because the electron density of the quinone in **1** is influenced by the coordinated ML$_n$ units, we conclude that the metal and quinone are electronically coupled, behavior exhibited in monometallic analogues supported by **NqMes**.[58] By extension, the electron density of ML$_n$ fragments coordinated to **1** should be sensitive to changes in the quinone (e.g., quinone reduction; vide infra).

Complexes **5a** and **5b** also displayed IR-active metal–carbonyl stretching modes, which allow measurement of the electron density at the coordinated metal centers. Because NHCs are strong σ donors, a CO ligand *trans* to the NHC will have a higher stretching frequency than a CO ligand with *cis* orientation.[85] The solid-state CO stretching bands *trans* and *cis* to the NHC units in **5a** occurred at 2089 and 2005 cm^{-1}, respectively, and were within the range observed for other NHC-supported [Rh(CO)$_2$Cl] complexes (*trans*: 2057–2093 cm^{-1}, *cis*: 1984–2006 cm^{-1}), including **NqMes**.[57,58,95,96] Similarly, the ν_{CO} values in KBr for congener **5b** at 2075 and 1989 cm^{-1} (*trans* and *cis*, respectively) were consistent with NHC-supported [Ir(CO)$_2$Cl] complexes (*trans*: 2055–2072 cm^{-1}, *cis*: 1971–1989 cm^{-1}), but at higher-than-average energies.[22,86,88,101]

A more quantitative measure of the electron donating ability of a ligand is its Tolman electronic parameter (TEP), which can be calculated from the stretching energies of metal carbonyl complexes it supports.[102] Work pioneered by Crabtree et al. and expanded by Nolan et al. and Plenio et al. allows determination of the TEP for NHC-supported [Ir(CO)$_2$Cl] complexes: $TEP = 0.847 \times \nu_{av}\ (Ir) + 336\ cm^{-1}$, where ν_{av} (Ir) is the average ν_{CO} value of the Ir-bound *cis* and *trans* carbonyl ligands.[86,87,89] Recently, Plenio and Wolf developed an equation for converting ν_{av} (Rh) values for NHC-supported [Rh(CO)$_2$Cl] complexes onto the same energy scale as [Ir(CO)$_2$Cl] complexes, whereby $\nu_{av}\ (Ir) = 0.8695 \times \nu_{av}\ (Rh) + 250.7\ cm^{-1}$, enabling comparison of the TEP values of these two congeners.[85] For complexes **5a** and **5b**, the average solid-state CO stretching energies ν_{av} are 2047 and 2032 cm^{-1}, respectively, with no significant difference between the solid- and solution-state measurements (Table 2). Using ν_{av} (**5a**) = 2047 cm^{-1}, the Ir-scaled value was calculated to be 2030.6 cm^{-1}. With ν_{av} values for both **5a** and **5b** on the same scale, their respective TEP values of 2055.9 and 2057.1 cm^{-1} were found to be nearly identical, that is, **1** donates electron density equally well to [Rh(CO)$_2$Cl] and [Ir(CO)$_2$Cl] fragments. Furthermore, the TEP values for **5a** and **5b** are within the range observed in NHC-supported [Rh(CO)$_2$Cl] and [Ir(CO)$_2$Cl] complexes (2046.7–2057.3 cm^{-1}), closely resembling that of

Table 2. Carbonyl stretching frequencies and Tolman electronic parameters.

	Solid-state[a]		Solution-state[b]		Reduced[c]	
	ν_{av} [cm^{-1}]	TEP [cm^{-1}]	ν_{av} [cm^{-1}]	TEP [cm^{-1}]	ν_{av} [cm^{-1}]	TEP [cm^{-1}]
5a	2047	2055.9	2048	2056.6	2034	2046
5b	2032	2057.1	2032	2057.1	2018	2045

[a] Average values for metal-carbonyl stretching modes (ν_{av}) and Tolman electronic parameters (TEP) obtained in KBr matrices. [b] Average values for metal-carbonyl stretching modes (ν_{av}) and Tolman electronic parameters (TEP) obtained in CH_2Cl_2 solution. [c] Values for one-electron reduced complexes of **5a** and **5b** obtained by IR spectroelectrochemistry in CH_2Cl_2 containing 0.1 M nBu$_4$NPF$_6$ (see Table 4 and accompanying discussion).

4,5-dichloro-1,3-bis(2,6-diisopropylphenyl)imidazolylidene (2055.1 cm^{-1}).[85,86]

To probe the variation of electron density of **1** in complexes thereof and to gain insight into how this redox-active ligand affects the electronics of coordinated ML_n units, we performed a series of electrochemical measurements on bis-azolium $[\mathbf{1}H_2][OTf]_2$ and complexes **2**–**5** (Table 3).[69] Cyclic voltammetry (CV) of $[\mathbf{1}H_2][OTf]_2$ in CH_3CN displayed two quasireversible peaks at +0.31 V and −0.66 V versus SCE,[103] assigned as the first[104] and second quinone reductions, respectively. Chronoamperometry (CA) confirmed that each peak corresponded to a one-electron process.[69] Because the second reduction occurs at −0.66 V in the dication of $[\mathbf{1}H_2][OTf]_2$, compounds comprising neutral **1** should exhibit only the first reduction within the solvent window, thus simplifying electrochemical analysis. Furthermore, the potential of the $QBI^{0/1-}$ couple should serve as a diagnostic tool for the variation of ligand electron density in complexes **2**–**5**: values approaching +0.31 V would suggest significant bis-azolium and, therefore, zwitterionic character.

Table 3. Electrochemical properties.[a]

	Metal oxidation			Ligand reduction		
	$E_{1/2}$ [V]	ΔE [V]	n	$E_{1/2}$ [V]	ΔE [V]	n
$[\mathbf{1}H_2][OTf]_2$[b]	–	–	–	0.31	0.12	1.05
2[c]	0.44	0.12	1.93	−0.48	0.18	0.91
3[c]	0.46	0.11	1.96	0.083	0.092	0.94
4a[c]	1.00	0.10	1.90	−0.40	0.088	0.94 1
4b[c]	0.97	0.10	1.94	−0.42	0.089	0.93
5a[c]	–	–	–	−0.31	0.13	0.90
5b[c]	–	–	–	−0.34	0.10	0.92

[a] $\Delta E = E_{pa} - E_{pc}$. n determined by chronoamperometry. [b] Measurements performed with 1 mM analyte and 0.1 M nBu_4NPF_6 in CH_3CN. [c] Measurements performed with 1 mM analyte and 0.1 M nBu_4NPF_6 in CH_2Cl_2.

Because we were interested in the effects of ligand reduction on coordinated ML_n fragments in complexes **2**–**5**, we sought to study the nature of the reduced ligand (i.e., $\mathbf{1}^-$). Although all attempts to characterize the electrochemical properties of **1** by CV resulted in rapid decomposition, reaction of **1** with a stoichiometric quantity of $CoCp_2$ in THF afforded a compound that exhibited a sharp, isotropic EPR signal at $g = 2.008$ (Figure 6A).[105] This value is consistent with those of other semiquinone radical anionic species[106,107] and the signal for $\mathbf{1}^-$ matched a simulated isotropic spectrum centered at $g = 2.008$ (Figure 6B). The absence of hyperfine coupling indicated that the spin density was localized primarily on the quinone moiety and leads us to suggest that reduction of the QBI linker in complexes **2**–**5** could increase the overall electron-donating ability of **1** without significantly altering the electronic topology of the NHC sites.

Complexes **2**–**5** exhibited $QBI^{0/1-}$ potentials that were indicative of the extent of metal–ligand interaction and correlated with the ν_{CO} (quinone) values. All complexes exhibited only one ligand reduction within the solvent window, and CA revealed these to be one-electron processes.[69] Quinone reduction in **2** and **3** occurred at −0.48 and +0.083 V (Table 3), the highest and lowest energies of all the complexes analyzed, respectively (Table 3). Complexes **4a** and **4b** displayed ligand reductions at −0.40 and −0.42 V, and the $QBI^{0/1-}$ couples for **5a** and **5b** were measured to be −0.31 and −0.34 V, respectively. Because the quinone reduction for **3** occurred at the lowest energy of the complexes studied, we believe its QBI core is the most electron-deficient and has zwitterionic character. The $QBI^{0/1-}$ couple observed in **5** is less negative than the analogous couples observed in **4** presumably due to the greater electron-withdrawing ability of $[M(CO)_2Cl]$ versus [M(cod)Cl]. Furthermore, the reductions in complexes **4b** and **5b** occurred at slightly higher energies than in their Rh congeners, reflecting the slightly diminished orbital overlap of Ir with **1**. Overall, the QBI reduction potentials agree well with the quinone stretching frequencies observed for complexes **2**–**5**, for which increasing ν_{CO} (quinone) correlated to lower $QBI^{0/1-}$ energies (**3** > **5a** > **5b** > **4a** > **4b** > **2**).

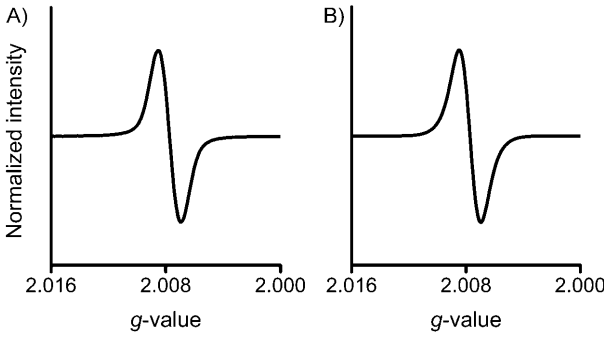

Figure 6. Experimental (A) and simulated (B) EPR spectra of $\mathbf{1}^+[CoCp_2]$ in THF.

After analyzing the $QBI^{0/1-}$ potentials in **2**–**5**, we compared the ML_n oxidation potentials to those of **BBI**-supported analogues to determine the electron-donating character of **1** and any metal–metal electronic coupling. Complexes **2**–**5** displayed only one metal-centered peak corresponding to two indistinguishable one-electron oxidations (for **2** and **3**, $Fe^{II/III}$; for **4** and **5**, $M^{I/II}$; Table 3), as judged by differential pulse voltammetry (DPV) and CA.[69] Ferrocene oxidation in **2** and **3** occurred at +0.44 and +0.46 V (Table 3), respectively, lower than for free FcN_3 and FcNCS (+0.59 and +0.72 V, respectively).[83] Because the $Fe^{II/III}$ couple in FcNCS shifts more upon adduct formation than that of FcN_3, **1** donates more electron density to the FcNCS units, an assessment supported by the reduction potentials for **2** and **3** (−0.48 and +0.083 V, respectively). Interestingly, the [M(cod)Cl] oxidations in **4a** and **4b** at +1.01 and +0.97 V, respectively, were similar to those of **BBI**-based Rh and Ir complexes.[29] No metal-based oxidations for complex **5a** or **5b** were observed within the solvent window, a result that is consistent with the electrochemical behavior of other known

NHC-supported $[M(CO)_2Cl]$ complexes (M = Rh and Ir).[60,85,87] On the basis of these findings, as well as the IR spectroscopic analyses of **5a** and **5b**, we conclude that **1** donates electron density in a similar manner to **BBI** or **IMes**. This finding suggests retention of imidazolylidene coordination chemistry.

Having shown that the electronic properties of **1** and its bimetallic complexes are consistent with those of other NHC-supported analogues, we sought to determine how changing the QBI oxidation state would affect the electron density at coordinated metal atoms. To study the extent of these metal–ligand interactions in **2**–**5**, we investigated the electronic impact of ML_n oxidation on the ditopic ligand and QBI reduction on the coordinated metal centers, respectively, by means of IR spectroelectrochemistry. We hypothesized that oxidation of the coordinated metals in **2**–**4** would render them more electron deficient and thus withdraw more electron density from **1**, affording an increase in the ν_{CO} (quinone) value (for **2** and **3**, see Scheme 7A; for **4a** and **4b**, see Scheme 7B). Alternatively, reducing the QBI in **5a** or **5b** should render the ligand more electron rich and therefore more donating, resulting in greater electron density within the $[M(CO)_2Cl]$ fragments and a decrease in the average ν_{CO} (M–CO) values ν_{av} (see Scheme 7C). This type of transformation would ultimately represent control over the TEP and, given the dependence of spectral properties and reactivity on the electron density of the metal center, any catalytic, electronic, or physical properties by extension.

We employed IR spectroelectrochemistry to measure the shift in ν_{CO} (quinone) for **2**–**4** (in CH_2Cl_2 containing 0.1 M nBu$_4$NPF$_6$) upon oxidation of the metal centers (Table 4).

Table 4. IR Spectroelectrochemical properties.[a]

	Metal oxidation[b]				Ligand reduction[c]		
	ν_{CO}	ν_{CO}^{ox}	$\Delta\nu_{CO}$		ν_{CO}	ν_{CO}^{red}	$\Delta\nu_{av}$
2	1662	1681	+19	**5a**	2088, 2008	2074, 1994	−14
3	1694	1704	+10	**5b**	2074, 1990	2060, 1976	−15
4a	1681	1689	+8				
4b	1678	1687	+9				

[a] All values in cm^{-1}. Measurements were performed on 10 mM analyte in CH_2Cl_2 with 0.1 M nBu$_4$NPF$_6$. [b] ν_{CO} and ν_{CO}^{red} correspond to the quinone stretching energies in the neutral and oxidized complexes, respectively; $\Delta\nu_{CO} = \nu_{CO}^{ox} - \nu_{CO}$. [c] ν_{CO} and ν_{CO}^{red} correspond to the metal-bound carbonyl stretching energies in the neutral and reduced complexes, respectively; $\Delta\nu_{av}$ is the average of the two $\Delta\nu_{CO}$ values ($\Delta\nu_{CO} = \nu_{CO}^{red} - \nu_{CO}$).

Oxidizing the ferrocene units in **2** afforded a 19 cm^{-1} increase in the quinone stretching energy, but shifts of $\leq$10 cm^{-1} were observed in **3** and **4**. Presumably, the smaller $\Delta\nu_{CO}$ (quinone) for **3** versus **2** reflects the linker geometry: direct metal–quinone interaction is possible across the coplanar triazene units in **2**, but not the orthogonal NCS moiety in **3**. Because the $\Delta\nu_{CO}$ (quinone) values for **3** and **4** were similar despite different structural and electronic features, we believe they are derived from the buildup of positive charge on the molecule. Thus, the $\Delta\nu_{CO}$ (quinone) $\approx$ 9 cm^{-1} in these systems arises mainly from the Coulombic impact of metal oxidation on ligand electron density, whereby direct metal–quinone coupling was relatively minor. However, the $\Delta\nu_{CO}$ (quinone) value of 19 cm^{-1} observed in **2** is consistent with a relatively significant metal–ligand electronic interaction. As observed in a **BBI** (R = *tert*-amyl) system, we believe the linkage geometry between the bis-NHC and coordinated metal atoms governs the metal–ligand interaction. Specifically, we propose that orthogonality precludes effective overlap (**III** and **3** and **4**), while coplanarity facilitates enhanced it (**II** and **2**).

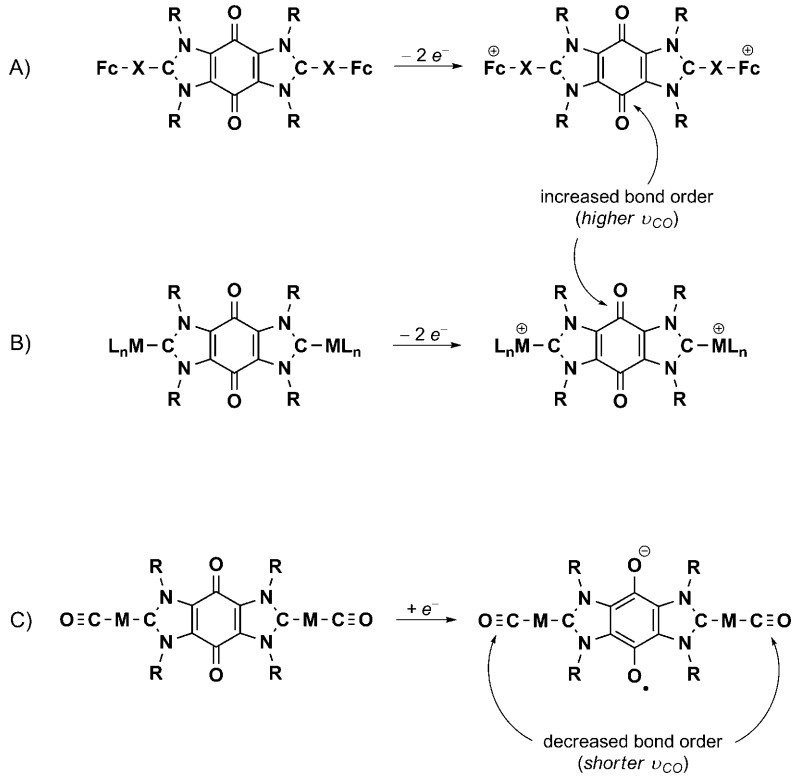

Scheme 7. Oxidation of A) Fc (X = N_3 and NCS for **2** and **3**, respectively) and B) [M(cod)Cl] units (M = Rh and Ir for **4a** and **4b**, respectively) decreases the electron density within the QBI, thus increasing the quinone bond strength and ν_{CO} (quinone). Conversely, reduction of the QBI (C) increases the electron density at the coordinated metal atoms (M = Rh and Ir for **5a** and **5b**, respectively), causing a decrease in the carbonyl bond order and ν_{CO}. R = mesityl.

Because oxidizing the ML_n units in **2–4** diminishes the QBI electron density and thus increases ν_{CO} (quinone), we reasoned that reducing the quinone moiety in **5a** and **5b** would afford more electron rich $[M(CO)_2Cl]$ units and lower the observed average carbonyl stretching energies ν_{av}. Indeed, reduction of **1** decreased ν_{av} for **5a** and **5b** by 14 and 15 cm^{-1}, respectively (see Figure 7 and Table 4), similar

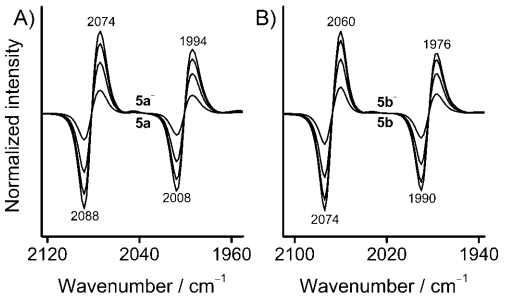

Figure 7. Normalized difference IR spectra at 60 s intervals showing the shift in ν_{CO} upon reduction ($E_{app} = -1.0$ V) of A) **5a**→**5a**$^-$ and B) **5b**→**5b**$^-$ in CH_2Cl_2 containing 10 mM analyte and 0.1 M n-Bu_4NPF_6.

to **NqMes**.[60] These ν_{av} shifts are interpreted as indicating C–O bonds weakened by increased electron density on the metal center, and reflect the greater electron donating ability of anionic **1**$^-$ versus neutral **1**. The TEP values for **5a**$^-$ and **5b**$^-$ of 2046 and 2045 cm^{-1} confirm enhanced ligand-donating ability upon reduction (Table 2), that is, **1**$^-$ is among the most electron donating NHCs (2046.7–2057.3 cm^{-1}).[85,86] Given that the spectroscopic and structural features of **5a** and **5b** are similar to those of other NHC-supported $[M(CO)_2Cl]$ complexes, we conclude that **1** retains the coordination chemistry of the **BBI** scaffold. Thus, **1** could be used as a structural replacement for **BBI** that enables tuning of the electron density at coordinated metal centers through changes in quinone redox state and facilitate redox-switchable control over the intrinsic properties of bis-NHC-supported complexes.

Conclusions

We have prepared quinobis(imidazolylidene) **1**, an electron-configurable bis-NHC in which two imidazolylidene units are linked by a redox active *p*-quinone in excellent yield after two steps. Treating **1** with FcN_3, FcNCS, and [M(cod)Cl] afforded complexes **2**, **3**, **4a** (M = Rh), or **4b** (M = Ir), respectively. Complexes **4a** and **4b** were converted to their $[M(CO)_2Cl]$ derivatives **5a** and **5b** upon reaction with excess CO(g). Because the NMR spectroscopic and structural features of these bimetallic species were similar to those of **BBI**-supported analogues, we believe that the coordination chemistry exhibited by the imidazolyidene units in **BBI** is retained in **1**, despite annulation to an electron-withdrawing quinone linker.

The quinone stretching energies and reduction potentials in **2–5** correlate with the relative electron-donating/withdrawing abilities of the ML_n fragments, whereby more electron deficient metals increase the ν_{CO} (quinone) value and the QBI reduction potential (**3** > **5a** > **5b** > **4a** > **4b** > **2**). Overall, these results indicate that the quinone in **1** was electronically perturbed upon ML_n binding. Further information on this interaction was obtained by IR spectroelectrochemistry, in which oxidizing the metal centers in **2–4** increased ν_{CO} (quinone) in accordance with the extent of NHC–ML_n overlap. Conversely, this interaction was also used to affect the electronic properties of coordinated metals, whereby reducing the QBI moiety increased the electron density on the metal center. Ligand reduction in **5a** and **5b** decreased the average ν_{CO} values by 14 and 15 cm^{-1}, and corresponding TEPs by 10 and 12 cm^{-1}, respectively. The similarity of these shifts is consistent with the observation that **1** donates equal electron density to $[Rh(CO)_2Cl]$ and $[Ir(CO)_2Cl]$.

Collectively, these results suggest that the metal–quinone electronic interaction in bimetallic complexes of **1** could be used as a practical means to increase the electron density at the ML_n units through quinone reduction. Because the imidazolylidene units in **1** exhibit similar structure/reactivity to those found in **BBI**s and analogous NHCs, despite the redox-active quinone linker, we believe **1** could be used to prepare derivatives with electroactive properties. Where **BBI**s have facilitated access to phosphorescent bimetallic complexes,[29] polymeric catalysts,[30] emissive and conductive polymers,[21,31–33] as well as self-assembled materials,[34,35] substitution with a redox-active bis-NHC like **1** could afford analogues whose intrinsic properties can be modulated by changing the ligand oxidation state.

Experimental Section

Materials and methods: Compounds **1–5** were prepared under an N_2 atmosphere by using dry-box or Schlenk techniques; all other syntheses were performed under ambient conditions. Azidoferrocene (FcN_3) was prepared as previously described.[83] Dichloromethane and toluene were distilled from CaH_2. THF was distilled from Na/benzophenone. Solvents were degassed by three consecutive freeze–pump–thaw cycles. All other reagents were used without further purification. ^1H, $^{13}C\{^1H\}$, and $^{19}F\{^1H\}$ NMR spectra were recorded on a Varian 300, 400, or 500 MHz spectrometer. Chemical shifts δ (in ppm) for ^1H and ^{13}C NMR are referenced to tetramethylsilane by using the residual solvent as an internal standard. For ^1H NMR: $CDCl_3$, $\delta = 7.24$ ppm; CD_2Cl_2, $\delta = 5.32$ ppm; CD_3CN, $\delta = 1.94$ ppm; C_6D_6, $\delta = 7.15$ ppm; [D$_6$]DMSO, $\delta = 2.49$ ppm; [D$_8$]THF, $\delta = 3.58$ ppm. For ^{13}C NMR: $CDCl_3$, $\delta = 77.0$ ppm; CD_2Cl_2, $\delta = 53.8$ ppm; CD_3CN, $\delta = 118.69$ ppm; C_6D_6, $\delta = 128.0$ ppm; [D$_6$]DMSO, $\delta = 39.5$ ppm; [D$_8$]THF, $\delta = 67.6$ ppm. Chemical shifts for ^{19}F NMR are referenced to $CFCl_3$ (0.00 ppm) as an external standard. Coupling constants are expressed in hertz. FTIR spectra were recorded on a Perkin-Elmer Spectrum BX system. For the $[M(CO)_2Cl]$ complexes, we attribute the ν_{CO} bands to the carbonyl ligands coordinated *cis* and *trans* to their respective NHC.[108] High-resolution mass spectra (HRMS) were obtained with a VG analytical ZAB2-E instrument (ESI or CI). EPR spectra were acquired on a Bruker continuous-wave X-band EPR spectrometer and simulated by using the integrated Simfonia software package. Elemental

analyses were performed by Columbia Analytical Labs (Tucson, AZ) or Atlantic Microlabs (Norcross, GA).

Electrochemistry: Electrochemical experiments were conducted on CH Instruments Electrochemical Workstations (series 660D and 700B) using a gas-tight, three-electrode cell under an atmosphere of dry nitrogen. Cells were equipped with gold working, tungsten counter-, and silver quasireference electrodes. Measurements were performed in dry CH_2Cl_2 with 0.1 M nBu$_4$NPF$_6$ electrolyte and decamethylferrocene (Fc*) internal standard. Differential pulse voltammetry measurements were performed with 50 mV pulse amplitudes and 2 mV data intervals. Chronoamperometry experiments were performed with a 25 μm-diameter Au ultramicroelectrode as working electrode to enable independent determination of D_0 and n by plotting $i(t)/i_{ss}$ versus $t^{-1/2}$ and using the Cottrell equation. Data deconvolution and fitting were performed with the Origin 8.0 software package. All reported potentials were determined at 100 mV s^{-1} scan rate and referenced to saturated calomel electrode (SCE) by shifting $(Fc^*)^{0/+}$ to −0.057 V (CH_2Cl_2) or −0.044 V (CH_3CN).[109]

1,1′,3,3′-Tetramesitylquinobis(imidazolium) dibromide ([1H$_2$][Br]$_2$): Bromanil (500 mg, 1.18 mmol) and *N*,*N*′-dimesitylformamidine[66] (1.30 g, 4.63 mmol) were dissolved in CH_3CN (25 mL) and the solution heated to 110 °C, resulting in gradual formation of a red precipitate. After 24 h, the mixture was cooled to room temperature. The precipitate was collected by vacuum filtration, washed with excess CH_3CN and Et_2O, and dried under vacuum to afford the desired product (880 mg, 1.07 mmol; 91 % yield) as a dark orange solid. M.p. 296 °C (decomp); ^{1}H NMR (500 MHz, [D$_6$]DMSO): δ = 10.17 (s, 2H), 7.14 (s, 8H), 2.31 (s, 12H), 2.19 (S, 24H); ^{13}C NMR (100 MHz, [D$_6$]DMSO): δ = 163.7, 141.2, 134.7, 130.7, 129.3, 128.8, 20.6, 17.8; IR (KBr): $\tilde{\nu}$ = 1708 cm^{-1} (C=O, quinone); HRMS calcd for $C_{44}H_{46}BrN_4O_2$ [M−Br]$^+$: 741.2804; found: 741.2811; elemental analysis (%) calcd for $C_{44}H_{48}Br_2N_4O_3$ ([**1**H$_2$][Br]$_2$·H$_2$O): C 62.86, H 5.75, N 6.66; found: C 62.96, H 5.61, N 6.58.

1,1′,3,3′-Tetramesitylquinobis(imidazolium) bis-triflate ([1H$_2$][OTf]$_2$): After [**1**H$_2$][Br]$_2$ (100 mg, 122 μmol) was suspended in CH_2Cl_2 (5 mL), MeOTf (0.10 mL, 0.91 mmol) was added, which resulted in the formation of a yellow suspensate. After 2 h, the precipitate was collected by vacuum filtration, washed with excess CH_2Cl_2 and Et_2O, and then dried under vacuum to afford the desired product (111 mg, 0.115 μmol; 94 % yield) as a yellow solid. M.p. 346 °C (decomp); ^{1}H NMR (400 MHz, CD_3CN): δ = 9.30 (s, 2H), 7.17 (s, 8H), 2.37 (s, 12H), 2.15 ppm (s, 24H); ^{13}C NMR (75 MHz, CD_3CN): δ = 164.9, 145.7, 143.7, 135.4, 131.8, 130.8, 129.2, 21.1, 17.8 ppm; ^{19}F NMR (376 MHz, CD_3CN): δ = −79.3 ppm; IR (KBr): $\tilde{\nu}$ = 1710 cm^{-1} (C=O, quinone); electrochemistry: $E_{1/2}$ = +0.31 V (first reduction, $\triangle E$ = 0.12 V, quasireversible, $D_0 = 8.0\times10^{-10}$ m^2 s^{-1}, n = 1.05); HRMS calcd for $C_{45}H_{46}F_3N_4O_5S$ [M−OTf]$^+$: 811.3148; found: 811.3141; elemental analysis (%) calcd for $C_{46}H_{46}F_6N_4O_8S_2$: C 57.49, H 4.82, N 5.83; found: C 57.38, H 4.72, N 5.90.

1,1′,3,3′-Tetramesitylquinobis(imidazolylidene) (1): [**1**H$_2$][Br]$_2$ (500 mg, 0.61 mmol) and NaN(SiMe$_3$)$_2$ (217 mg, 1.19 mmol) were dissolved in THF (30 mL) and the mixture was stirred at room temperature. After 30 min, this green mixture was filtered through a 0.4 μm PTFE filter and then concentrated under vacuum to afford the desired product (320 mg, 0.48 mmol; 79 % yield) as a dark green solid. This compound must be stored in the cold and under an inert atmosphere to prevent decomposition. M.p. 82 °C (decomp); ^{1}H NMR (500 MHz, C_6D_6): δ = 6.92 (2 s, 8H), 2.09 (s, 24H), 2.03 ppm (s, 12H); ^{13}C NMR (100 MHz, [D$_8$]THF): δ = 232.6, 168.0, 138.5, 137.0, 134.9, 132.8, 129.6, 21.0, 18.0 ppm; IR (KBr): $\tilde{\nu}$ = 1676 cm^{-1} (C=O, quinone); elemental analysis (%) calcd for $C_{44}H_{48}N_4O_4$ [**1**·2H$_2$O]: C 75.83, H 6.94, N 8.04; found: C 76.32, H 6.88, N 7.84.

[(FcN$_3$)$_2$(1)] (2): A solution of FcN$_3$ (71 mg, 0.28 mmol) in THF (2 mL) was added to a solution of **1** (93 mg, 0.14 mmol) in THF (3 mL), and the resulting mixture stirred at room temperature, resulting in gradual formation of a cloudy, dark brown-red solution. After 16 h, the solvent was removed under reduced pressure and the remaining residue was washed with Et_2O (4×3 mL). Removal of the residual solvent under vacuum afforded the desired product (85 mg, 76 μmol; 54 % yield) as a brick red solid. ^{1}H NMR (400 MHz, $CDCl_3$): δ = 6.94 (s, 8H), 4.03 (t, J = 2.0, 4H), 3.97 (s, 8H), 3.91 (t, J = 2.0, 4H), 2.31 (s, 12H), 2.13 ppm (s, 24H); ^{13}C NMR (75 MHz, $CDCl_3$): δ = 164.9, 150.5, 138.7, 134.5, 131.9, 129.6, 125.0, 104.1, 69.2, 67.4, 63.5, 21.2, 18.1 ppm; IR (KBr): $\tilde{\nu}$ = 1662 cm^{-1} (C=O, quinone); electrochemistry: $E_{1/2}$ = +0.44 V ($Fe^{II/III}$, ΔE = 0.12 V, quasireversible, $D_0 = 8.2\times10^{-10}$ m^2 s^{-1}, n = 1.93), −0.48 V ($QBI^{0/-}$, ΔE = 0.18 V, quasireversible, $D_0 = 8.5\times10^{-10}$ m^2 s^{-1}, n = 0.91); HRMS calcd for $C_{64}H_{63}N_{10}O_2Fe_2$ [M^+]: 1115.3839; found: 1115.3834; elemental analysis (%) calcd for $C_{64}H_{62}N_{10}O_2Fe_2$: C 68.94, H 5.61, N 12.56; found: C 69.26, H 5.48, N 12.69.

[(FcNCS)$_2$(1)] (3): A solution of FcNCS (20 mg, 82 μmol) in toluene (2 mL) was added to a solution of **1** (27 mg, 41 μmol) in toluene (2 mL), and the resulting mixture was stirred at room temperature, resulting in the gradual formation of a cloudy, dark brown-red solution. After 16 h, the solvent was removed under reduced pressure and the remaining residue was washed with Et_2O (4×3 mL). Removal of the residual solvent under vacuum afforded the desired product (24 mg (21 μmol, 51 % yield) as a dark brown solid. ^{1}H NMR (400 MHz, $CDCl_3$): δ = 6.93 (brs, 8H), 4.83 (brs, 4H), 3.97 (brs, 4H), 3.75 (s, 10H), 2.33 (s, 24H), 2.23 ppm (s, 12H); ^{13}C NMR (100 MHz, CD_2Cl_2): δ = 171.1, 141.2, 135.44, 135.37, 130.0, 129.8, 129.5, 128.8, 126.3, 68.6, 68.4, 65.8, 65.7, 65.5, 65.3, 64.7, 60.3, 31.9, 30.0, 29.7, 29.3, 22.7, 21.2, 21.0, 20.8, 18.7, 14.2, 14.1 ppm; IR (KBr): $\tilde{\nu}$ = 1692 cm^{-1} (C=O, quinone); electrochemistry: $E_{1/2}$ = +0.46 V ($Fe^{II/III}$, ΔE = 0.11 V, quasireversible, $D_0 = 1.3\times10^{-9}$ m^2 s^{-1}, n = 1.96), +0.083 V ($QBI^{0/-}$, ΔE = 0.092 V, quasireversible, $D_0 = 1.3\times10^{-9}$ m^2 s^{-1}, n = 0.94); HRMS calcd for $C_{66}H_{64}N_6O_2S_2Fe_2$ [M^+]: 1148.32255; found: 1148.3223; elemental analysis (%) calcd for $C_{66.25}H_{62.5}Cl_{0.5}N_6O_2S_2Fe_2$ (**3**·0.25 CH_2Cl_2): C 68.11, H 5.39, N 7.19; found: C 67.99, H 5.56, N 7.18.

[{Rh(cod)Cl}$_2$(1)] (4a): Bis-NHC **1** (70 mg, 0.10 mmol) and [{Rh(cod)Cl}$_2$] (51 mg, 0.10 mmol) were dissolved in THF (10 mL). The resulting brown solution was stirred for 12 h at room temperature, during which the color gradually changed to dark red-brown. The residual solvent was then removed under reduced pressure and the resulting dark red-brown solid was washed with Et_2O to remove any unconsumed [{Rh(cod)Cl}$_2$]. Subsequent purification by chromatography (Al_2O_3, first 3/1 hexanes/EtOAc to remove impurities then CH_2Cl_2) afforded the desired product (80 mg, 69 μmol; 69 % yield) as a dark brown powder. ^{1}H NMR (400 MHz, $CDCl_3$): δ = 7.03 (s, 4H), 6.95 (s, 4H), 4.52 (brs, 4H), 3.26 (brs, 4H), 2.35 (s, 12H) overlaps 2.32 (d, J = 9.6, 12H), 1.90 (d, J = 8.0, 12H), 1.76–1.61 (br m, 8H), 1.60–1.46 ppm (br m, 8H); ^{13}C NMR (125 MHz, $CDCl_3$): δ = 201.0 (d, J = 53.1), 164.5, 139.38, 139.36, 136.9, 136.6, 133.6, 133.5, 133.2, 131.3, 131.2, 130.3, 130.1, 128.4, 128.2, 98.44, 98.39, 68.6, 68.5, 68.4, 32.51, 32.46, 28.03, 28.01, 21.2, 19.9, 19.8, 18.3 ppm; IR (KBr): $\tilde{\nu}$ = 1680 cm^{-1} (C=O, quinone); electrochemistry: $E_{1/2}$ = +1.00 V ($Rh^{I/II}$, ΔE = 0.10 V, quasireversible, $D_0 = 1.1\times10^{-9}$ m^2 s^{-1}, n = 1.90), −0.40 V ($QBI^{0/-}$, ΔE = 0.088 V, quasireversible, $D_0 = 1.1\times10^{-9}$ m^2 s^{-1}, n = 0.94); HRMS calcd for $C_{60}H_{68}Cl_2N_4O_2Rh_2$ [M^-]: 1152.2829; found: 1152.2835; elemental analysis (%) calcd for $C_{60}H_{68}N_4O_2Rh_2$: C 62.45, H 5.94, N 4.86; found: C 62.20, H 5.70, N 4.70.

[{Ir(cod)Cl}$_2$(1)] (4b): Bis-NHC **1** (35 mg, 53 μmol) and [{Ir(cod)Cl}$_2$] (36 mg, 54 μmol) were dissolved in THF (5 mL). The resulting brown-red mixture was stirred for 16 h at room temperature, during which the color gradually changed to dark brown. The residual solvent was then removed under reduced pressure and the resulting dark brown solid was washed with Et_2O to remove any unconsumed [{Ir(cod)Cl}$_2$]. Subsequent purification by chromatography (Al_2O_3, first 3/1 hexanes/EtOAc to remove impurities then CH_2Cl_2) afforded the desired product (45 mg, 34 μmol; 64 % yield) as a dark brown-black powder. ^{1}H NMR (300 MHz, CD_2Cl_2): δ = 7.03 (s, 4H), 7.00 (s, 4H), 4.15 (brs, 4H), 3.04 (brs, 4H), 2.38 (s, 12H), 2.25 (d, J = 4.8, 12H), 1.99 (d, J = 3.0, 12H), 1.57 ppm (brs, 8H); ^{13}C NMR (125 MHz, $CDCl_3$). δ = 195.3, 164.9, 139.28, 136.5, 136.2, 133.5, 133.32, 133.28, 131.04, 131.00, 130.3, 130.14, 130.07, 129.9, 129.7, 128.5, 128.3, 128.2, 128.0, 86.2, 86.1, 52.7, 52.5, 52.3, 52.1, 33.35, 33.33, 28.5, 21.4, 21.2, 21.0, 20.0, 19.8, 19.7, 19.6, 18.7, 18.42, 18.40, 18.2 ppm; IR (KBr): $\tilde{\nu}$ = 1678 cm^{-1} (C=O, quinone); electrochemistry: $E_{1/2}$ = +0.97 V ($Ir^{I/II}$, ΔE = 0.10 V, quasireversible, $D_0 = 9.8\times10^{-10}$ m^2 s^{-1}, n = 1.94), −0.42 V ($QBI^{0/-}$, ΔE = 0.089 V, quasireversible, $D_0 = 9.9\times10^{-10}$ m^2 s^{-1}, n = 0.93); HRMS calcd for $C_{60}H_{68}ClN_4O_2Ir_2$ [M^+]: 1297.42838; found: 1297.4271; elemental analysis (%) calcd for $C_{60}H_{68}Cl_2N_4O_2Ir_2$: C 54.08, H 5.14, N 4.20; found: C 53.63, H 5.01, N 4.01.

[{Rh(CO)$_2$Cl}$_2$(1)] (5a): Complex **4a** (25 mg, 22 μmol) was dissolved in CH_2Cl_2 (5 mL) and sparged with CO(g) at room temperature until the solvent had evaporated. The residue was washed with hexanes (4×5 mL) under a static CO atmosphere, then dried under vacuum to afford the desired product (21 mg, 20 μmol; 91% yield) as a light orange powder. ^{1}H NMR (300 MHz, $CDCl_3$): δ=6.97 (s, 8H), 2.33 (s, 12H), 2.11 (s, 24H); ^{13}C NMR (75 MHz, $CDCl_3$): δ=193.0 (d, J=45.8), 184.0 (d, J=54.7), 182.0 (d, J=72.7), 164.1, 140.2, 134.1, 132.5, 131.2, 129.8, 21.3, 18.6; IR (KBr): $\tilde{\nu}$=2089 (IrCO, *trans*), 2005 (IrCO, *cis*), 1688 cm^{-1}(C=O, quinone). IR (CH_2Cl_2, NaCl): $\tilde{\nu}$=2089 (IrCO, *trans*), 2005 (IrCO, *cis*), 1686 cm^{-1} (C=O, quinone); electrochemistry: $E_{1/2}$=−0.31 V (QBI$^{0/-}$, ΔE=0.13 V, quasireversible, D_0=9.0×10^{-10} m^{2}s^{-1}, n=0.90); HRMS calcd for $C_{48}H_{44}N_4O_6Rh_2Cl_2$ [M^-]: 1048.0748; found: 1048.0754; elemental analysis (%) calcd for $C_{48}H_{44}Cl_2N_4O_6Rh_2$: C 54.93, H 4.23, N 5.34; found: C 54.70, H 4.20, N 4.90.

[{Ir(CO)$_2$Cl}$_2$(1)] (5b): Complex **4b** (20 mg, 15 μmol) was dissolved in CH_2Cl_2 (5 mL) and sparged with CO(g) at room temperature until the solvent had evaporated. The residue was washed hexanes (4×5 mL) under a static CO atmosphere, then dried under vacuum to afford the desired product (17 mg, 14 μmol; 93% yield) as a light orange powder. ^{1}H NMR (300 MHz, $CDCl_3$): δ=6.96 (s, 8H), 2.33 (s, 12H), 2.11 ppm (s, 24H); ^{13}C NMR (75 MHz, $CDCl_3$): δ=188.7, 178.8, 167.7, 164.1, 140.4, 134.0, 132.2, 131.0, 129.8, 21.3, 18.6 ppm; IR (KBr): $\tilde{\nu}$=2075 (IrCO, *trans*), 1989 (IrCO, *cis*), 1686 cm^{-1} (C=O, quinone); IR (CH_2Cl_2, NaCl): $\tilde{\nu}$=2074 (IrCO, *trans*), 1990 (IrCO, *cis*), 1688 cm^{-1} (C=O, quinone); electrochemistry: −0.34 V (QBI$^{0/-}$, ΔE=0.10 V, quasireversible, D_0=9.3×10^{-10} m^{2}s^{-1}, n=0.92); HRMS calcd for $C_{48}H_{44}N_4O_6Ir_2Cl$ [M^+]: 1193.22024; found: 1193.2188; elemental analysis (%) calcd for $C_{48}H_{44}Cl_2N_4O_6Ir_2$: C 46.94, H 3.61, N 4.56; found: C 46.80, H 3.30, N 4.50.

Acknowledgements

We are grateful to the NSF (CHE-0645563 and CHE-0749571 for C.W.B. and J.L.S., respectively), the ONR (N00014-08-1-0729), the Arnold and Mabel Beckman Foundation, the Sloan Foundation, and the Robert A. Welch Foundation (F-1621 and F-1018 to C.W.B and J.L.S, respectively) for their generous financial support. Funding for the EPR spectrometer was supplied by the NSF (CHE-0639239). C.W.B. is a Cottrell Scholar of the Research Corporation.

[1] C. Schneider, *Angew. Chem.* **2009**, *121*, 2116–2118; *Angew. Chem. Int. Ed.* **2009**, *48*, 2082–2084.
[2] A. J. Esswein, A. S. Veige, D. G. Nocera, *J. Am. Chem. Soc.* **2005**, *127*, 16641–16651.
[3] N. Marion, S. P. Nolan, *Acc. Chem. Res.* **2008**, *41*, 1440–1449.
[4] J. M. Praetorius, C. M. Crudden, *Dalton Trans.* **2008**, 4079–4094.
[5] S. Díez-González, S. P. Nolan, *Acc. Chem. Res.* **2008**, *41*, 349–358.
[6] S. Würtz, F. Glorius, *Acc. Chem. Res.* **2008**, *41*, 1523–1533.
[7] F. J. Gómez, N. E. Kamber, N. M. Deschamps, A. P. Cole, P. A. Wender, R. M. Waymouth, *Organometallics* **2007**, *26*, 4541–4545.
[8] M. F. Lappert, *J. Organomet. Chem.* **2005**, *690*, 5467–5473.
[9] B. E. Ketz, A. P. Cole, R. M. Waymouth, *Organometallics* **2004**, *23*, 2835–2837.
[10] E. Peris, R. H. Crabtree, *Coord. Chem. Rev.* **2004**, *248*, 2239–2246.
[11] D. Bourissou, O. Guerret, F. P. Gabbaï, G. Bertrand, *Chem. Rev.* **2000**, *100*, 39–91.
[12] A. J. Arduengo III, *Acc. Chem. Res.* **1999**, *32*, 913–921.
[13] W. A. Herrmann, K. Köcher, *Angew. Chem.* **1997**, *119*, 2156–2182; *Angew. Chem. Int. Ed. Engl.* **1997**, *36*, 2162–2187.
[14] F. E. Hahn, M. C. Jahnke, *Angew. Chem.* **2008**, *120*, 3166–3216; *Angew. Chem. Int. Ed.* **2008**, *47*, 3122–3172.
[15] R. J. Lowry, M. K. Veige, O. Clément, K. A. Abboud, I. Ghiviriga, A. S. Veige, *Organometallics* **2008**, *27*, 5184–5195.
[16] L. H. Gade, S. Bellemin-Laponnaz, *Top Organomet. Chem.* **2007**, *21*, 117–157.
[17] J. A. Mata, M. Poyatos, E. Peris, *Coord. Chem. Rev.* **2007**, *251*, 841–859.
[18] M. Poyatos, J. A. Mata, E. Peris, *Chem. Rev.* **2009**, *109*, 3677–3707.
[19] F. Boeda, S. P. Nolan, *Annu. Rep. Prog. Chem. Sect. B* **2008**, *104*, 184–210.
[20] D. M. Khramov, A. J. Boydston, C. W. Bielawski, *Angew. Chem.* **2006**, *118*, 6332–6335; *Angew. Chem. Int. Ed.* **2006**, *45*, 6186–6189.
[21] A. J. Boydston, K. A. Williams, C. W. Bielawski, *J. Am. Chem. Soc.* **2005**, *127*, 12496–12497.
[22] E. Mas-Marzá, J. A. Mata, E. Peris, *Angew. Chem.* **2007**, *119*, 3803–3805; *Angew. Chem. Int. Ed.* **2007**, *46*, 3729–3731.
[23] M. Poyatos, W. McNamara, C. Incarvito, E. Clot, E. Peris, R. H. Crabtree, *Organometallics* **2008**, *27*, 2128–2136.
[24] F. J.-B. dit Dominique, H. Gornitzka, A. Sournia-Saquet, C. Hemmert, *Dalton Trans.* **2009**, 340–352.
[25] M. Raynal, C. S. J. Cazin, C. Vallée, H. Olivier-Bourbigou, P. Braunstein, *Chem. Commun.* **2008**, 3983–3985.
[26] R. B. Bedford, M. Betham, D. W. Bruce, A. A. Danopoulos, R. M. Frost, M. Hird, *J. Org. Chem.* **2006**, *71*, 1104–1110.
[27] B. Liu, W. Chen, S. Jin, *Organometallics* **2007**, *26*, 3660–3667.
[28] U. J. Scheele, S. Dechert, F. Meyer, *Inorg. Chim. Acta* **2006**, *359*, 4891–4900.
[29] A. G. Tennyson, E. L. Rosen, M. S. Collins, V. M. Lynch, C. W. Bielawski, *Inorg. Chem.* **2009**, *48*, 6924–6933.
[30] B. Karimi, P. F. Akhavan, *Chem. Commun.* **2009**, 3750–3752.
[31] D. J. Coady, B. C. Norris, D. M. Khramov, A. G. Tennyson, C. W. Bielawski, *Angew. Chem. Int. Ed.* **2009**, *121*, 5289–5292; *Angew. Chem. Int. Ed.* **2009**, *48*, 5187–5190.
[32] A. G. Tennyson, J. W. Kamplain, C. W. Bielawski, *Chem. Commun.* **2009**, 2124–2126.
[33] A. J. Boydston, J. D. Rice, M. D. Sanderson, O. L. Dykhno, C. W. Bielawski, *Organometallics* **2006**, *25*, 6087–6098.
[34] C. Radloff, F. E. Hahn, T. Pape, R. Fröhlich, *Dalton Trans.* **2009**, 7215–7222.
[35] F. E. Hahn, C. Radloff, T. Pape, A. Hepp, *Organometallics* **2008**, *27*, 6408–6410.
[36] J. K. Lassila, D. Herschlag, *Biochemistry* **2008**, *47*, 12853–12859.
[37] J. G. Zalatan, I. Catrina, R. Mitchell, P. K. Grzyska, P. J. O'Brien, D. Herschlag, A. C. Hengge, *J. Am. Chem. Soc.* **2007**, *129*, 9789–9798.
[38] M. H. Sazinsky, S. J. Lippard, *Acc. Chem. Res.* **2006**, *39*, 558–566.
[39] J. S. Valentine, P. A. Doucette, S. Z. Potter, *Annu. Rev. Biochem.* **2005**, *74*, 563–593.
[40] J. S. Valentine, P. J. Hart, *Proc. Natl. Acad. Sci. USA* **2003**, *100*, 3617–3622.
[41] A. J. Bard, L. R. Faulkner, *Electrochemical Methods: Fundamentals and Applications*, 2nd ed., Wiley, New York, **2001**.
[42] N. G. Connelly, W. E. Geiger, *Chem. Rev.* **1996**, *96*, 877–910.
[43] C. K. A. Gregson, V. C. Gibson, N. J. Long, E. L. Marshall, P. J. Oxford, A. J. P. White, *J. Am. Chem. Soc.* **2006**, *128*, 7410–7411.
[44] M. Süßner, H. Plenio, *Angew. Chem.* **2005**, *117*, 7045–7048; *Angew. Chem. Int. Ed.* **2005**, *44*, 6885–6888.
[45] H. Plenio, C. Aberle, *Chem. Eur. J.* **2001**, *7*, 4438–4446.
[46] H. Plenio, C. Aberle, Y. A. Shihadeh, J. M. Lloris, R. Martínez-Máñez, T. Pardo, J. Soto, *Chem. Eur. J.* **2001**, *7*, 2848–2861.
[47] H. Plenio, C. Aberle, *Angew. Chem.* **1998**, *110*, 1467–1470; *Angew. Chem. Int. Ed.* **1998**, *37*, 1397–1399.
[48] A. M. Allgeier, C. A. Mirkin, *Angew. Chem.* **1998**, *110*, 936–952; *Angew. Chem. Int. Ed.* **1998**, *37*, 894–908.
[49] I. M. Lorkovic, R. R. Duff, Jr., M. S. Wrighton, *J. Am. Chem. Soc.* **1995**, *117*, 3617–3618.
[50] B. Baeza, L. Casarrubios, P. Ramíirez-Lopez, M. Gómez-Gallego, M. A. Sierra, *Organometallics* **2009**, *28*, 956–959.
[51] G. Gachot, P. Pellon, T. Roisnel, D. Lorcy, *J. Organomet. Chem.* **2009**, *694*, 2531–2535.
[52] F. Ba, N. Cabon, F. R.-L. Guen, P. L. Poul, N. L. Poul, Y. L. Mest, S. Golhen, B. Caro, *Organometallics* **2008**, *27*, 6396–6399.
[53] S. L. Caldwell, J. B. Gilroy, R. Jain, E. Crawford, B. O. Patrick, R. G. Hicks, *Can. J. Chem.* **2008**, *86*, 976–981.

[54] D. Guo, J. K. McCusker, *Inorg. Chem.* **2007**, *46*, 3257–3274.
[55] T. Hirao, *Coord. Chem. Rev.* **2002**, *226*, 81–91.
[56] A. J. Boydston, C. W. Bielawski, *Dalton Trans.* **2006**, 4073–4077.
[57] D. M. Khramov, E. L. Rosen, V. M. Lynch, C. W. Bielawski, *Angew. Chem.* **2008**, *120*, 2299–2302; *Angew. Chem. Int. Ed.* **2008**, *47*, 2267–2270.
[58] M. D. Sanderson, J. W. Kamplain, C. W. Bielawski, *J. Am. Chem. Soc.* **2006**, *128*, 16514–16515.
[59] D. M. Khramov, V. M. Lynch, C. W. Bielawski, *Organometallics* **2007**, *26*, 6042–6049.
[60] E. R. Rosen, C. D. Varnado, A. G. Tennyson, D. M. Khramov, J. W. Kamplain, D. H. Sung, P. J. Creswell, V. M. Lynch, C. W. Bielawski, *Organometallics*, DOI: 10.1021/om900698x.
[61] D. H. Sung, J. W. Kamplain, M. D. Sanderson, C. W. Bielawski, unpublished results.
[62] L. Delaude, *Eur. J. Inorg. Chem.* **2009**, 1681–1699.
[63] V. Nair, S. Bindu, V. Sreekumar, *Angew. Chem.* **2004**, *116*, 5240–5245; *Angew. Chem. Int. Ed.* **2004**, *43*, 5130–5135.
[64] B. Bildstein, M. Malaun, H. Kopacka, K. Wurst, M. Mitterböck, K.-H. Ongania, G. Opromolla, P. Zanello, *Organometallics* **1999**, *18*, 4325–4336.
[65] "Coupling" and "interaction" are used to describe how changing in the electronic properties of a metal center influences those of the ligand (and vice versa).
[66] K. M. Kuhn, R. H. Grubbs, *Org. Lett.* **2008**, *10*, 2075–2077.
[67] Substituting chloranil for bromanil afforded the corresponding bis-azolium chloride salt, albeit in slightly lower yield (87%). All attempts to generate the bis-NHC from this precursor have been unsuccessful.
[68] P. D. Vu, A. J. Boydston, C. W. Bielawski, *Green Chem.* **2007**, *9*, 1158–1159.
[69] Supporting Information available: ^{1}H and ^{13}C NMR spectra; syntheses of FcNCS and [**1**H$_2$][Cl]$_2$, ORTEP of [**1**H$_2$][OTf]$_2$; X-ray crystallographic details, data tables, and CIF files for [**1**H$_2$][OTf]$_2$, **1**–**3**, **4a**, and **5a**; electrochemical figures (CV, DPV, CA) for [**1**H$_2$][OTf]$_2$ and **2**–**5**; spectroelectrochemical spectra for **2**–**4**.
[70] M. S. Jeletic, M. T. Jan, I. Ghiviriga, K. A. Abboud, A. S. Veige, *Dalton Trans.* **2009**, 2764–2776.
[71] A. J. Boydston, C. S. Pecinovsky, S. T. Chao, C. W. Bielawski, *J. Am. Chem. Soc.* **2007**, *129*, 14550–14551.
[72] H. V. Huynh, Y. Han, J. H. H. Ho, G. K. Tan, *Organometallics* **2006**, *25*, 3267–3274.
[73] S. Saravanakumar, A. I. Oprea, M. K. Kindermann, P. G. Jones, J. Heinicke, *Chem. Eur. J.* **2006**, *12*, 3143–3154.
[74] F. E. Hahn, M. C. Jahnke, V. Gomez-Benitez, D. Morales-Morales, T. Pape, *Organometallics* **2005**, *24*, 6458–6463.
[75] H. V. Huynh, J. H. H. Ho, T. C. Neo, L. L. Koh, *J. Organomet. Chem.* **2005**, *690*, 3854–3860.
[76] A. A. Danopoulos, S. Winston, T. Gelbrich, M. B. Hursthouse, R. P. Tooze, *Chem. Commun.* **2002**, 482–483.
[77] J. A. Wright, A. A. Danopoulos, W. B. Motherwell, R. J. Carroll, S. Ellwood, J. Saßmannshausen, *Eur. J. Inorg. Chem.* **2006**, 4857–4865.
[78] X. Hu, I. Castro-Rodriguez, K. Meyer, *Organometallics* **2003**, *22*, 3016–3018.
[79] F. E. Hahn, L. Wittenbecher, R. Boese, D. Bläser, *Chem. Eur. J.* **1999**, *5*, 1931–1935.
[80] D. M. Khramov, A. J. Boydston, C. W. Bielawski, *Org. Lett.* **2006**, *8*, 1831–1834.
[81] A. J. Arduengo III, H. V. R. Dias, R. L. Harlow, M. Kline, *J. Am. Chem. Soc.* **1992**, *114*, 5530–5534.
[82] D. M. Khramov, C. W. Bielawski, *J. Org. Chem.* **2007**, *72*, 9407–9417.
[83] A. G. Tennyson, D. M. Khramov, C. D. Varnado, Jr., P. T. Creswell, J. W. Kamplain, V. M. Lynch, C. W. Bielawski, *Organometallics* **2009**, *28*, 5142–5147.
[84] By indistinguishable, we do not mean identical, merely that the component processes cannot be resolved: for two identical, noninteracting redox processes, the statistical separation is 36 mV due to entropic factors.
[85] S. Wolf, H. Plenio, *J. Organomet. Chem.* **2009**, *694*, 1487–1492.
[86] R. A. Kelly III, H. Clavier, S. Giudice, N. M. Scott, E. D. Stevens, J. Bordner, I. Samardjiev, C. D. Hoff, L. Cavallo, S. P. Nolan, *Organometallics* **2008**, *27*, 202–210.
[87] a) S. Leuthäußer, D. Schwarz, H. Plenio, *Chem. Eur. J.* **2007**, *13*, 7195–7203; b) T. Vorfalt, S. Leuthäußer, H. Plenio, *Angew. Chem.* **2009**, *121*, 5293–5296; *Angew. Chem. Int. Ed.* **2009**, *48*, 5191–5194.
[88] G. Altenhoff, R. Goddard, C. W. Lehmann, F. Glorius, *J. Am. Chem. Soc.* **2004**, *126*, 15195–15201.
[89] A. R. Chianese, X. Li, M. C. Janzen, J. W. Faller, R. H. Crabtree, *Organometallics* **2003**, *22*, 1663–1667.
[90] M. Iglesias, D. J. Beetstra, B. Kariuki, K. J. Cavell, A. Dervisi, I. A. Fallis, *Eur. J. Inorg. Chem.* **2009**, 1913–1919.
[91] F. Ullah, M. K. Kindermann, P. G. Jones, J. Heinicke, *Organometallics* **2009**, *28*, 2441–2449.
[92] A. Bittermann, P. Härter, E. Herdtweck, S. D. Hoffmann, W. A. Herrmann, *J. Organomet. Chem.* **2008**, *693*, 2079–2090.
[93] H. M. Peng, R. D. Webster, X. Li, *Organometallics* **2008**, *27*, 4484–4493.
[94] A. Zanardi, R. Corberán, J. A. Mata, E. Peris, *Organometallics* **2008**, *27*, 3570–3576.
[95] S. Burling, M. F. Mahon, S. P. Reade, M. K. Whittlesey, *Organometallics* **2006**, *25*, 3761–3767.
[96] P. Bazinet, T.-G. Ong, J. S. O'Brien, N. Lavoie, E. Bell, G. P. A. Yap, I. Korobkov, D. S. Richeson, *Organometallics* **2007**, *26*, 2885–2895.
[97] P. R. Campodónico, A. Aizman, R. Contreras, *Chem. Phys. Lett.* **2009**, *471*, 168–173.
[98] C. Vazquez, J. C. Calabrese, D. A. Dixon, J. S. Miller, *J. Org. Chem.* **1993**, *58*, 65–81.
[99] E. C. M. Chen, W. E. Wentworth, *J. Chem. Phys.* **1975**, *63*, 3183–3191.
[100] F. A. Cotton, G. Wilkinson, C. A. Murillo, M. Bochmann, *Advanced Inorganic Chemistry*, 6th ed., Wiley, New York, **1999**.
[101] M. Iglesias, D. J. Beetstra, A. Stasch, P. N. Horton, M. B. Hursthouse, S. J. Coles, K. J. Cavell, A. Dervisi, I. A. Fallis, *Organometallics* **2007**, *26*, 4800–4809.
[102] C. A. Tolman, *Chem. Rev.* **1977**, *77*, 313–348.
[103] All potentials are reported relative to saturated calomel electrode (SCE).
[104] Qualitative evidence that the higher potential peak is a ligand-based reduction came upon addition of the Fc* reference, whereupon a deep blue color developed, indicative of Fc* oxidation.
[105] This chemical reduction appears quasireversible: **1**$^{-}$ can be generated and isolated, then treated with $FcBF_4$ to afford an NMR spectrum featuring a signal at $\delta = 6.92$ ppm, characteristic of neutral QBI **1**.
[106] Y. Song, G. R. Buettner, S. Parkin, B. A. Wagner, L. W. Robertson, H.-J. Lehmler, *J. Org. Chem.* **2008**, *73*, 8296–8304.
[107] H. Wu, D. Zhang, G. Zhang, D. Zhu, *J. Org. Chem.* **2008**, *73*, 4271–4274.
[108] Because no symmetry operation exchanges the *cis* and *trans* carbonyl ligands on one metal center, they will not be vibrationally coupled and will therefore exhibit independent stretching modes.
[109] I. Noviandri, K. N. Brown, D. S. Fleming, P. T. Gulyas, P. A. Lay, A. F. Masters, L. Phillips, *J. Phys. Chem. B* **1999**, *103*, 6713–6722.

Received: July 7, 2009
Published online: November 27, 2009

